Proceedings of the EuroGNC 2013, 2nd CEAS Specialist Conference
on Guidance, Navigation & Control, Delft University of Technology,
Delft, The Netherlands, April 10-12, 2013

Rotorcraft system identification: an integrated time-frequency domain approach

Marco Bergamasco and Marco Lovera

Abstract The problem of rotorcraft system identification is considered and a novel, two step technique is proposed, which combines the advantages of time domain and frequency domain methods. In the first step, the identification of a black-box model using a subspace model identification method is carried out, using a technique which can deal with data generated under feedback; subsequently, in the second step, *a-priori* information on the model structure is enforced in the identified model using an $\mathscr{H}_\infty$ model matching method. A simulation study is used to illustrate the proposed approach.

1 Introduction

The problem of system identification of helicopter aeromechanics has been studied extensively in the last few decades, as identification has been known for a long time as a viable approach to the derivation of control-oriented dynamic models in the rotorcraft field (see for example the recent books [21, 12] and the references therein). Model accuracy is becoming more and more important, as progressively stringent requirements are being imposed on rotorcraft control systems: as the required control bandwidth increases, accurate models become a vital part of the design problem.

In the system identification literature, on the other hand, one of the main novelties of the last two decades has been the development of the so-called Subspace Model Identification (SMI) methods (see for example the books [22, 25]), which have proven extremely successful in dealing with the estimation of state space models for Multiple-Inputs Multiple-Outputs (MIMO) systems. Surprisingly enough, even though SMI can be effectively exploited in dealing with MIMO modelling problems,

Marco Bergamasco
Dipartimento di Elettronica e Informazione, Politecnico di Milano,
e-mail: bergamasco@elet.polimi.it

Marco Lovera
Dipartimento di Elettronica e Informazione, Politecnico di Milano e-mail: lovera@elet.polimi.it

until recently these methods have received limited attention from the rotorcraft community, with the partial exception of some contributions such as [24, 7, 16]). SMI methods are particularly well suited for rotorcraft problems, for a number of reasons. First of all, the subspace approach can deal in a very natural way with MIMO problems; in addition, all the operations performed by subspace algorithms can be implemented with numerically stable and efficient tools from numerical linear algebra. Finally, information from separate data sets (such as generated during different experiments on the system, *i.e.*, different test flights) can be merged in a very simple way into a single state space model. Recently, see [15], the interest in SMI for helicopter model identification has been somewhat revived and the performance of subspace methods has been demonstrated on flight test data. However, so far only methods and tools which go back 10 to 15 years in the SMI literature (such as the MOESP algorithm of [23] and the bootstrap-based method for uncertainty analysis of [8]) have been considered. Therefore, the further potential benefits offered by the latest developments in the field have not been fully exploited. Among other things, present-day approaches can provide:

- unbiased model estimates from data generated during closed-loop operation, as is frequently the case in experiments for rotorcraft identification (see, *e.g.*, [9, 11]);
- the possibility to quantify model uncertainty using analytical expressions for the variance of the estimates instead of relying on computational statistics (see [9]);
- the direct estimation of continuous-time models from (possibly non-uniformly) sampled input-output data (see [6] and the references therein).

Some preliminary results in the application of continuous-time SMI to the rotorcraft problem have been presented in [5].

The only, well known, downside of the SMI approach to state space model identification, on the other hand, is the impossibility to impose a fixed basis to the state space representation. This, in turn, implies that it is hard to impose a parameterisation to the state space matrices in this framework, and therefore recovering physically-motivated models is a challenging problem. This, to date, prevents the successful application of SMI methods to the problem of initialising iterative methods for the identification of structured state space representations and constitutes a major stumbling block for the application of such methods in communities in which physically motivated models represent the current practice.

In this paper the problem of bridging the gap between ”unstructured” models obtained using SMI and structured ones deriving from flight mechanics is addressed as an input-output model matching one, in terms of the $\mathscr{H}_\infty$ norm of the difference between the two models (see also [3]). The solution of the problem is then computed using recent results in non-smooth optimisation techniques, see [1], which yield effective computational tools (see [10]).

In view of the above discussion, this paper has the following objectives. First, a set of methods suitable for time-domain, continuous-time identification of rotorcraft dynamics using SMI is presented. The proposed technique can deal with data generated in closed-loop operation as it does not require restrictive assumptions in this sense. Subsequently, a frequency-domain $\mathscr{H}_\infty$ approach to the problem of deriving a structured model from the unstructured one is proposed. Finally, the achievable

model accuracy is illustrated by means of simulation results for a full-scale helicopter.

The paper is organised as follows. In Section 2 the problem statement is given and some definitions are provided. Section 3 provides a summary of the proposed two-step approach. Finally, some simulation results are presented in Section 4 to illustrate the performance of the proposed method.

2 Problem statement and preliminaries

Consider the linear, time-invariant continuous-time system

$$\mathscr{M}_s(\lambda): \begin{cases} \dot{x}(t) = A(\lambda)x(t) + B(\lambda)u(t) + w(t),\ x(0) = x_0 \\ y(t) = C(\lambda)x(t) + D(\lambda)u(t) + v(t) \end{cases} \tag{1}$$

where $x \in \mathbb{R}^n$, $u \in \mathbb{R}^m$ and $y \in \mathbb{R}^p$ are, respectively, the state, input and output vectors and $w \in \mathbb{R}^n$ and $v \in \mathbb{R}^p$ are the process and the measurement noise, respectively, with covariance given by

$$E\left\{ \begin{bmatrix} w(t_1) \\ v(t_1) \end{bmatrix} \begin{bmatrix} w(t_2) \\ v(t_2) \end{bmatrix}^T \right\} = \begin{bmatrix} Q & S \\ S^T & R \end{bmatrix} \delta(t_2 - t_1).$$

The system matrices $A(\lambda)$, $B(\lambda)$, $C(\lambda)$, and $D(\lambda)$ are dependent on the constant parameter vector $\lambda \in \mathbb{R}^{n_\lambda}$ such that $(A(\lambda), C(\lambda))$ is observable and $(A(\lambda), [B(\lambda), Q^{1/2}])$ is controllable.

Assume now that a dataset $\{u(t_i), y(t_i)\}$, $i \in [1, N]$ of sampled input/output data (possibly associated with a non equidistant sequence of sampling instants) obtained from system (1) is available. Then, the problem is to provide an estimate of the parameter λ on the basis of the available data. Note that unlike most identification techniques, in this setting incorrelation between u and w, v is not required, so that this approach is viable also for systems operating under feedback.

In the following Sections a number of definitions will be used, which are summarised hereafter for the sake of clarity (see, *e.g.*, [26, 13, 17, 2] for further details).

Definition 1. (**Laguerre basis**) Let $\mathscr{L}_2(0, \infty)$ denote the space of square integrable and Lebesgue measurable functions of time $0 < t < \infty$. Consider the first order all-pass (inner) transfer function

$$w(s) = \frac{s - a}{s + a}, \tag{2}$$

$a > 0$. $w(s)$ generates the family of Laguerre filters, defined as

$$\mathscr{L}_i(s) = w^i(s)\mathscr{L}_0(s) = \sqrt{2a}\frac{(s-a)^i}{(s+a)^{i+1}}. \tag{3}$$

Denote with $\ell_i(t)$ the impulse response of the i-th Laguerre filter. Then, it can be shown that the set

$$\{\ell_0, \ell_1, \ldots, \ell_i, \ldots\} \tag{4}$$

is an orthonormal basis of $\mathscr{L}_2(0,\infty)$, *i.e.*, all signals in $\mathscr{L}_2(0,\infty)$ can be represented by means of the set of their projections on the Laguerre basis.

Definition 2. ($\mathscr{H}_\infty$ **norm**) Consider an asymptotically stable, linear time-invariant system with transfer function $G(s)$. Then the $\mathscr{H}_\infty$ norm of the system is defined as

$$\|G\|_\infty = \sup_{\alpha>0} \left\{ \sup_{\omega} \bar{\sigma}\left(G(\alpha + j\omega)\right) \right\} = \sup_{\omega} \bar{\sigma}\left(G(j\omega)\right), \tag{5}$$

where $\bar{\sigma}$ is the maximum singular value.

Identifiability is an important issue in system identification problems; for the purpose of this study we adopt the following definitions:

Definition 3. (**Local identifiability**) Let $\lambda^o \in \Lambda \subset \mathbb{R}^{n_\lambda}$, the model structure is said to be locally identifiable in λ^o if $\forall \lambda_1, \lambda_2$ in the neighborhood of λ^o it holds that

$$\mathscr{M}_s(\lambda_1) = \mathscr{M}_s(\lambda_2) \Rightarrow \lambda_1 = \lambda_2.$$

Definition 4. (**Global identifiability**) The model structure $\mathscr{M}_s(\lambda)$ is said to be globally identifiable if it is locally identifiable $\forall \lambda \in \Lambda$, *i.e.*, over the entire parameter space.

In the following the model structure $\mathscr{M}_s(\lambda)$ is considered globally identifiable.

3 An integrated time-frequency domain approach

The problem formulated in the previous Section can be faced using a two-steps approach: in the first step a black-box model is identified using a continuous-time SMI method, which can deal with data generated under feedback but generates an "unstructured" model; in the subsequent step *a-priori* information on the model structure is enforced in the model using an $\mathscr{H}_\infty$ model matching method.

In Section 2 the gray-box model $\mathscr{M}_s(\lambda)$ was introduced, while a generic "unstructured" black-box model $\mathscr{M}_{ns}$ can be described as the linear time-invariant system

$$\mathscr{M}_{ns} : \begin{cases} \dot{x}(t) = \hat{A}x(t) + \hat{B}u(t) + w(t),\ x(0) = x_0 \\ y(t) = \hat{C}x(t) + \hat{D}u(t) + v(t) \end{cases} \tag{6}$$

where x, u, y, w, and v are defined as in Section 2. The system matrices $\hat{A}$, $\hat{B}$, $\hat{C}$ and $\hat{D}$ have been estimated from a dataset $\{u(t_i), y(t_i)\}$, $i \in [1,N]$ of sampled input/output data using the continuous-time predictor-based subspace model identification algorithm introduced in the Section 3.1. Suppose $\mathscr{M}_{ns}$ belonging to the same model structure of $\mathscr{M}_s(\lambda)$, and that (1) and (6) describe the same system with different state space basis. Therefore the problem becomes to provide estimates of λ such that the

input-output behaviors of $\mathscr{M}_{ns}$ and $\mathscr{M}_s(\lambda)$ are equivalent under some criterion, and it is faced using an $\mathscr{H}_\infty$ approach described in Section 3.2.

3.1 Continuous-time predictor-based subspace model identification

3.1.1 From continuous-time to discrete-time using Laguerre projections

The main issue in the application of subspace model identification methods to continuous-time model identification is the need of computing the high order derivatives of input-output measurements arising from the continuous-time data equation. This problem can be faced using a method, based on the results first presented in [19, 17], and further expanded in [14, 18], that transforms a continuous-time system and signals to their discrete-time representations. First note that under the assumptions stated in the previous section, (6) can be written in innovation form as

$$\begin{aligned} \dot{x}(t) &= Ax(t) + Bu(t) + Ke(t) \\ y(t) &= Cx(t) + Du(t) + e(t) \end{aligned} \tag{7}$$

and it is possible to apply the results of [19] to derive a discrete-time equivalent model, as follows. Note that the notation $\hat{(\cdot)}$ has been dropped for clarity. Consider the first order inner function $w(s)$ defined in (2) and apply to the input u, the output y and the innovation e of (7) the transformations

$$\begin{aligned} \tilde{u}(k) &= \int_0^\infty \ell_k(t)u(t)dt \\ \tilde{y}(k) &= \int_0^\infty \ell_k(t)y(t)dt \\ \tilde{e}(k) &= \int_0^\infty \ell_k(t)e(t)dt, \end{aligned} \tag{8}$$

where $\tilde{u}(k) \in \mathbb{R}^m$, $\tilde{e}(k) \in \mathbb{R}^p$ and $\tilde{y}(k) \in \mathbb{R}^p$. Then (see [19] for details) the transformed system has the state space representation

$$\begin{aligned} \xi(k+1) &= A_o\xi(k) + B_o\tilde{u}(k) + K_o\tilde{e}(k),\ \xi(0) = 0 \\ \tilde{y}(k) &= C_o\xi(k) + D_o\tilde{u}(k) + \tilde{e}(k) \end{aligned} \tag{9}$$

where the state space matrices are given by

$$\begin{aligned} A_o &= (A - aI)^{-1}(A + aI) \\ B_o &= \sqrt{2a}(A - aI)^{-1}B \\ K_o &= \sqrt{2a}(I - C(A - aI)^{-1}K)^{-1}(A - aI)^{-1}K \\ C_o &= -\sqrt{2a}C(A - aI)^{-1} \\ D_o &= D - C(A - aI)^{-1}B. \end{aligned} \tag{10}$$

It is worth to underline that in this context k is not a time index, but refers to the projection of the signals onto the k-th basis function.

3.1.2 Predictor-based subspace model identification

In this Section a summary of the continuous-time PBSID algorithm proposed in [4, 6], called CT-PBSID$_o$, is provided, and its implemention is discussed. More precisely, starting from system (7), a sketch of the derivation of a PBSID-like approach to the estimation of the state space matrices A_o, B_o, C_o, D_o, K_o is presented. Considering the sequence of sampling instants t_i, $i = 1, \ldots, N$, the input u, the output y and the innovation e of (7) are subjected to the transformations

$$\begin{aligned} \tilde{u}_i(k) &= \int_0^\infty \ell_k(\tau) u(t_i+\tau) d\tau \\ \tilde{y}_i(k) &= \int_0^\infty \ell_k(\tau) y(t_i+\tau) d\tau \\ \tilde{e}_i(k) &= \int_0^\infty \ell_k(\tau) e(t_i+\tau) d\tau \end{aligned} \tag{11}$$

(or to the equivalent ones derived from (8)), where $\tilde{u}_i(k) \in \mathbb{R}^m$, $\tilde{e}_i(k) \in \mathbb{R}^p$ and $\tilde{y}_i(k) \in \mathbb{R}^p$. Then (see [19] for details) the transformed system has the state space representation

$$\begin{aligned} \xi_i(k+1) &= A_o \xi_i(k) + B_o \tilde{u}_i(k) + K_o \tilde{e}_i(k),\ \xi_i(0) = x(t_i) \\ \tilde{y}_i(k) &= C_o \xi_i(k) + D_o \tilde{u}_i(k) + \tilde{e}_i(k) \end{aligned} \tag{12}$$

where the state space matrices are given by (10).

Letting now

$$\tilde{z}_i(k) = \left[\tilde{u}_i^T(k)\ \tilde{y}_i^T(k)\right]^T$$

and

$$\begin{aligned} \bar{A}_o &= A_o - K_o C_o \\ \bar{B}_o &= B_o - K_o D_o \\ \widetilde{B}_o &= \left[\bar{B}_o\ K_o\right], \end{aligned}$$

system (12) can be written in predictor form as

$$\begin{aligned} \xi_i(k+1) &= \bar{A}_o \xi_i(k) + \widetilde{B}_o \tilde{z}_i(k),\ \xi_i(0) = x(t_i) \\ \tilde{y}_i(k) &= C_o \xi_i(k) + D_o \tilde{u}_i(k) + \tilde{e}_i(k), \end{aligned} \tag{13}$$

to which the PBSID$_{opt}$ algorithm, summarised hereafter, can be applied to compute estimates of the state space matrices A_o, B_o, C_o, D_o, K_o. To this purpose note that iterating $p-1$ times the projection operation (i.e., propagating $p-1$ forward in the

index k the first of equations (13), where p is the so-called past window length) one gets

$$\begin{aligned}\xi_i(k+2) &= \bar{A}_o^2\xi_i(k) + \left[\bar{A}_o\widetilde{B}_o\ \widetilde{B}_o\right]\begin{bmatrix}\tilde{z}_i(k)\\ \tilde{z}_i(k+1)\end{bmatrix}\\ &\vdots\\ \xi_i(k+p) &= \bar{A}_o^p\xi_i(k) + \mathscr{K}^p Z_i^{0,p-1}\end{aligned} \tag{14}$$

where

$$\mathscr{K}^p = \left[\bar{A}_o^{p-1}\widetilde{B}_0\ \ldots\ \widetilde{B}_o\right] \tag{15}$$

is the extended controllability matrix of the system in the transformed domain and

$$Z_i^{0,p-1} = \begin{bmatrix}\tilde{z}_i(k)\\ \vdots\\ \tilde{z}_i(k+p-1)\end{bmatrix}.$$

Under the considered assumptions, $\bar{A}_o$ has all the eigenvalues inside the open unit circle, so the term $\bar{A}_o^p\xi_i(k)$ is negligible for sufficiently large values of p and we have that

$$\xi_i(k+p) \simeq \mathscr{K}^p Z_i^{0,p-1}.$$

As a consequence, the input-output behaviour of the system is approximately given by

$$\begin{aligned}\tilde{y}_i(k+p) &\simeq C_o\mathscr{K}^p Z_i^{0,p-1} + D_o\tilde{u}_i(k+p) + \tilde{e}_i(k+p)\\ &\vdots\\ \tilde{y}_i(k+p+f) &\simeq C_o\mathscr{K}^p Z_i^{f,p+f-1} + D_o\tilde{u}_i(k+p+f) +\\ &\quad + \tilde{e}_i(k+p+f),\end{aligned} \tag{16}$$

so that introducing the vector notation

$$\begin{aligned}Y_i^{p,f} &= \left[\tilde{y}_i(k+p)\ \tilde{y}_i(k+p+1)\ \ldots\ \tilde{y}_i(k+p+f)\right]\\ U_i^{p,f} &= \left[\tilde{u}_i(k+p)\ \tilde{u}_i(k+p+1)\ \ldots\ \tilde{u}_i(k+p+f)\right]\\ E_i^{p,f} &= \left[\tilde{e}_i(k+p)\ \tilde{e}_i(k+p+1)\ \ldots\ \tilde{e}_i(k+p+f)\right]\\ \Xi_i^{p,f} &= \left[\xi_i(k+p)\ \xi_i(k+p+1)\ \ldots\ \xi_i(k+p+f)\right]\\ \bar{Z}_i^{p,f} &= \left[Z_i^{0,p-1}\ Z_i^{1,p}\ \ldots\ Z_i^{f,p+f-1}\right]\end{aligned} \tag{17}$$

equations (14) and (16) can be rewritten as

$$\begin{aligned}\Xi_i^{p,f} &\simeq \mathscr{K}^p \bar{Z}_i^{p,f} \\ Y_i^{p,f} &\simeq C_o \mathscr{K}^p \bar{Z}_i^{p,f} + D_o U_i^{p,f} + E_i^{p,f}.\end{aligned} \tag{18}$$

Considering now the entire dataset for $i = 1, \ldots, N$, the data matrices become

$$\begin{aligned}Y^{p,f} = [&\tilde{y}_1(k+p) \ldots \tilde{y}_N(k+p) \ldots \\ &\tilde{y}_1(k+p+f) \ldots \tilde{y}_N(k+p+f)],\end{aligned} \tag{19}$$

and similarly for $U_i^{p,f}$, $E_i^{p,f}$, $\Xi_i^{p,f}$ and $\bar{Z}_i^{p,f}$. The data equations (18), in turn, are given by

$$\begin{aligned}\Xi^{p,f} &\simeq \mathscr{K}^p \bar{Z}^{p,f} \\ Y^{p,f} &\simeq C_o \mathscr{K}^p \bar{Z}^{p,f} + D_o U^{p,f} + E^{p,f}.\end{aligned} \tag{20}$$

From this point on, the algorithm can be developed along the lines of the discrete-time PBSID$_{opt}$ method, i.e., by carrying out the following steps. Considering $p = f$, estimates for the matrices $C_o \mathscr{K}^p$ and D_o are first computed by solving the least-squares problem

$$\min_{C_o \mathscr{K}^p, D_o} \| Y^{p,p} - C_o \mathscr{K}^p \bar{Z}^{p,p} - D_o U^{p,p} \|_F, \tag{21}$$

where by $\| \cdot \|_F$ we denote the Frobenius norm of a matrix. Defining now the extended observability matrix Γ^p as

$$\Gamma^p = \begin{bmatrix} C_o \\ C_o \bar{A}_o \\ \vdots \\ C_o \bar{A}_o^{p-1} \end{bmatrix} \tag{22}$$

and noting that the product of Γ^p and $\mathscr{K}^p$ can be written as

$$\Gamma^p \mathscr{K}^p \simeq \begin{bmatrix} C_o \bar{A}^{p-1} \widetilde{B}_o & \ldots & C_o \widetilde{B}_o \\ 0 & \ldots & C_o \bar{A} \widetilde{B}_o \\ \vdots & & \\ 0 & \ldots & C_o \bar{A}^{p-1} \widetilde{B}_o \end{bmatrix}, \tag{23}$$

such product can be computed using the estimate $\widehat{C_o \mathscr{K}^p}$ of $C_o \mathscr{K}^p$ obtained by solving the least squares problem (21).

Recalling now that

$$\Xi^{p,p} \simeq \mathscr{K}^p \bar{Z}^{p,p} \tag{24}$$

it also holds that

$$\Gamma^p \Xi^{p,p} \simeq \Gamma^p \mathscr{K}^p \bar{Z}^{p,p}. \tag{25}$$

Therefore, computing the singular value decomposition

$$\Gamma^p \mathscr{K}^p \bar{Z}^{p,p} = U \Sigma V^T \tag{26}$$

an estimate of the state sequence can be obtained as

$$\widehat{\Xi}^{p,p} = \Sigma_n^{1/2} V_n^T = \Sigma_n^{-1/2} U_n^T \Gamma^p \mathscr{K}^p \bar{Z}^{p,p}, \tag{27}$$

from which, in turn, an estimate of C_o can be computed by solving the least squares problem

$$\min_{C_o} \| Y^{p,p} - \widehat{D}_o U^{p,p} - C_o \widehat{\Xi}^{p,p} \|_F. \tag{28}$$

The final steps consist of the estimation of the innovation data matrix $E^{p,p}$

$$E^{p,p} = Y^{p,p} - \widehat{C}_o \widehat{\Xi}^{p,p} - \widehat{D}_o U^{p,p} \tag{29}$$

and of the entire set of the state space matrices for the system in the transformed domain, which can be obtained by solving the least squares problem

$$\min_{A_o, B_o, K_o} \| \widehat{\Xi}^{p+1,p} - A_o \widehat{\Xi}^{p,p-1} - B_o U^{p,p-1} - K_o E^{p,p-1} \|_F. \tag{30}$$

The state space matrices of the original continuous-time system can then be retrieved by inverting the (bilinear) transformations (10).

3.2 From unstructured to structured models with an $\mathscr{H}_\infty$ approach

Suppose that the linear continuous-time time-invariant system $\mathscr{M}_{ns}$ has been estimated from a dataset of sampled input/output data using the CT-PBSID$_o$ algorithm presented in the previous Section. Consider now the model class $\mathscr{M}_s(\lambda)$ introduced in Section 1. $\mathscr{M}_{ns}$ and $\mathscr{M}_s(\lambda)$ should have the same input-output behavior. This problem can be faced in a computationally effective way by defining the input-output operators associated with $\mathscr{M}_{ns}$ and $\mathscr{M}_s(\lambda)$ and seeking the values of the parameters corresponding to the solution of the optimisation problem

$$\lambda^\star = \arg\min_{\lambda} \| \mathscr{M}_{ns} - \mathscr{M}_s(\lambda) \| \tag{31}$$

for a suitably chosen norm. In the linear time-invariant case, the input-output operators can be represented as the transfer functions $\hat{G}_{ns}(s)$ and $G_s(s;\lambda)$ and the $\mathscr{H}_\infty$ norm is considered, so that the model matching problem can be recast as

$$\lambda^\star = \arg\min_{\lambda} \| \hat{G}_{ns}(s) - G_s(s;\lambda) \|_\infty. \tag{32}$$

Note that the open-loop dynamics of a helicopter is unstable in most flight conditions and so the $\mathscr{H}_\infty$ norm is undefined. In this case the eigenvalues of $\mathscr{M}_s(\lambda)$ and $\mathscr{M}_{ns}$ are shifted on the real axis by a suitable value μ as follows

$$\tilde{G}_s(s;\lambda) = C(\lambda)((s-\mu)I - A(\lambda))^{-1}B(\lambda) + D(\lambda) \tag{33}$$

$$\tilde{G}_{ns}(s) = \hat{C}((s-\mu)I - \hat{A})^{-1}\hat{B} + \hat{D}, \tag{34}$$

where μ is chosen such that all eigenvalues of $\mathscr{M}_{ns}$ have negative real part. Then the model matching problem is reformulated as

$$\lambda^\star = \arg\min_{\lambda} \|\tilde{G}_{ns}(s) - \tilde{G}_s(s;\lambda)\|_\infty. \tag{35}$$

As mentioned in the Introduction, this is a non-convex, non-smooth optimisation problem, which has been studied extensively in recent years in the framework of the fixed-structured controller design problem and for which reliable computational tools (see [10]) are presently available.

4 Simulation study: model identification for the BO-105 helicopter

The simulation example considered in this paper is based on the BO-105 helicopter. Possibly it is the most studied helicopter in the rotorcraft system identification literature. The BO-105 is a light, twin-engine, multi-purpose utility helicopter.

It is considered in forward flight at 80 knots, a flight condition which corresponds to unstable dynamics, with the aim of demonstrating the identification of a nine-DOF state-space model with test data extracted from a simulator based on the nine-DOF model from [20]. As described in the cited reference, the model includes the classical six-DOF and some additional states to account for some additional effects, namely:

- the BO-105 exhibits highly coupled body-roll and rotor-flapping responses; their interaction is represented in the model with a dynamic equation that describes the flapping dynamics using the cyclic controls.
- A second order dipole is appended to the model of roll rate response to lateral stick in order to account for the effect of lead-lag rotor dynamics.

Therefore, the simulator includes a nine-DOF linear model including the six-DOF quasi steady dynamics, the flapping equations and the lead-lag dynamics modelled with a complex dipole. Delays at the input of the model are also taken into account in the simulation, though they are not estimated. The state vector and the trim values are

$$x = \begin{bmatrix} u\ v\ w\ p\ q\ r\ \phi\ \theta\ a_{1s}\ b_{1s}\ x_1\ x_2 \end{bmatrix}$$

and, respectively,

$$u_0 = 40 \text{ m/s}, \quad v_0 = 3 \text{ m/s}, \quad w_0 = -5 \text{ m/s}, \quad \phi_0 = 0 \text{ rad}, \quad \theta_0 = 0 \text{ rad}. \tag{36}$$

In details, the state vector includes the longitudinal flapping a_{1s}, the lateral flapping b_{1s} and two state variables x_1 and x_2, coming from the lead-lag dynamics complex dipole. The corresponding equations of motion are

$$
\begin{aligned}
\dot{u} &= X_u u + X_w w + X_p p + (X_q - w_0) q + v_0 r - g\theta + X_{\delta_{lon}} \delta_{lon} + X_{\delta_{col}} \delta_{col} \\
\dot{v} &= Y_v v + Y_w w + (Y_p + w_0) p + Y_q q + (Y_r - u_0) r - g\phi + Y_{\delta_{lat}} \delta_{lat} + Y_{\delta_{col}} \delta_{col} \\
\dot{w} &= Z_u u + Z_w w + (Z_p - v_0) p + u_0 q + Z_{\delta_{col}} \delta_{col} \\
\dot{p} &= L_u u + L_v v + L_w w + L_q q + L_{\delta_{b_{1s}}} b_{1s} + L_{\delta_{lon}} \delta_{lon} + L_{\delta_{ped}} \delta_{ped} + L_{\delta_{col}} \delta_{col} \\
\dot{q} &= M_v v + M_w w + M_p p + M_r r + M_{\delta_{a_{1s}}} a_{1s} + M_{\delta_{ped}} \delta_{ped} + M_{\delta_{col}} \delta_{col} \\
\dot{r} &= N_v v + N_w w + N_q q + N_r r + N_{\delta_{lon}} \delta_{lon} + N_{\delta_{lat}} \delta_{lat} + N_{\delta_{ped}} \delta_{ped} + N_{\delta_{col}} \delta_{col} \\
\dot{\phi} &= p \\
\dot{\theta} &= q \\
\dot{a}_{1s} &= -q - \frac{1}{\tau_f} a_{1s} + \frac{K_{a_{1s}}}{\tau_f} \delta_{lon}, \\
\dot{b}_{1s} &= -p - \frac{1}{\tau_f} b_{1s} + \frac{K_{b_{1s}}}{\tau_f} \delta_{lat} + K_{x_1} x_1 + K_{x_2} x_2 \\
\dot{x}_1 &= x_2 \\
\dot{x}_2 &= C_1 x_1 + C_2 x_2 + \delta_{lat}.
\end{aligned}
\tag{37}
$$

Finally, the output vector is

$$
y = \left[u \; v \; w \; p \; q \; r \; a_x \; a_y \; a_z \; \phi \; \theta \right],
$$

where

$$
\begin{aligned}
a_x &= \dot{u} + w_0 q - v_0 r + g\theta \\
a_y &= \dot{v} - w_0 p + u_0 r - g\phi \\
a_z &= \dot{w} + v_0 p - u_0 q,
\end{aligned}
$$

i.e., the state variables related to quasi-steady dynamics and the linear accelerations are measured. Considering (37), λ contains the stability derivatives, the control derivatives, the flapping and lead-lag rotor dynamics parameters, for a total of 47 parameters.

The identification experiment is performed in closed-loop because of the instability of the model, with the helicopter operating under feedback from an LQG controller tuned in order to maintain the helicopter close enough to trim to justify the identification of a linear model. In the experiment, additive perturbations have been applied to the input variables (δ_{lat},δ_{lon},δ_{ped},δ_{col}) computed by the controller; in particular, all the channels have been excited in the same experiment with pseudorandom binary signals with a duration of 60 s and a dwell time of 0.8 s. The perturbation of the control inputs has a 1% amplitude and the sampling time is 0.008s. For the purpose of the present preliminary study, measurement noise has not been included in the simulated data. The parameters of the algorithm presented in the previous Section have been chosen as $p = 40$ and $a = 45$. The obtained results are illustrated in Table 1.

As can be seen from the Table, the CT-PBSID$_o$ algorithm is able to identify the dynamics of the system with a slight loss of accuracy at high frequency.

	Simulator				Identified Model (CT-PBSID$_o$)			
	Real	Imag	Omega	Zeta	Real	Imag	Omega	Zeta
Pitch phugoid	0.119	0.278	0.302	-0.394	0.119	0.278	0.302	-0.394
Dutch roll	-0.571	2.546	2.609	0.219	-0.571	2.546	2.609	0.219
Roll/flapping	-9.904	7.740	12.569	0.788	-9.901	7.7399	12.568	0.788
Lead-Lag	-0.868	15.567	15.592	0.0557	-0.867	15.566	15.590	0.0556
Spiral	-0.0510				-0.0507			
Pitch$_1$	-0.448				-0.448			
Pitch$_2$	-5.843				-5.844			
Long. flapping	-15.930				-15.901			

Table 1 Comparison between simulator and black-box identified eigenvalues.

The study in the reconstruction of the above described structured state-space representation has been carried out by applying the approach presented in Section 3 to estimate the relevant parameters. In order to evaluate the performance of the proposed method the relative estimation error is defined as follows

$$\lambda_{err} = \frac{\lambda^0 - \bar{\lambda}}{\lambda^0}, \tag{38}$$

where $\hat{\lambda}$ and λ^0 are respectively the estimated and the actual value of the parameter λ. In this example the relative errors of the estimated physical parameters in (37) are below 0.03%. It is clear from Table 2, where the eigenvalues of the real system and the identified gray-box model are shown, that using *a-priori* information, *i.e.*, exploting the model structure, the estimation accuracy increases.

	Simulator				Identified Model (Gray-box)			
	Real	Imag	Omega	Zeta	Real	Imag	Omega	Zeta
Pitch phugoid	0.119	0.278	0.302	-0.394	0.119	0.278	0.302	-0.394
Dutch roll	-0.571	2.546	2.609	0.219	-0.571	2.546	2.609	0.219
Roll/flapping	-9.904	7.740	12.569	0.788	-9.903	7.740	12.568	0.788
Lead-Lag	-0.868	15.567	15.592	0.0557	-0.868	15.566	15.590	0.557
Spiral	-0.0510				-0.0507			
Pitch$_1$	-0.448				-0.448			
Pitch$_2$	-5.843				-5.843			
Long. flapping	-15.930				-15.929			

Table 2 Comparison between simulator and gray-box identified eigenvalues.

Finally, a time-domain validation of the identified models has been also carried out, by measuring the simulation accuracy of the models in response to a doublet input signal on each input channel. The input sequence used in the validation experiment is illustrated in Figure 1, while the time history for two of the outputs (u and w) is presented in Figure 2. Again, even though the open-loop system is unstable, the simulated outputs obtained from the identified models (dashed lines: black-box; cross: gray-box) match very well the ones computed from the nine-DOF model (solid lines).

In quantitative terms, considering the root mean square error, defined as

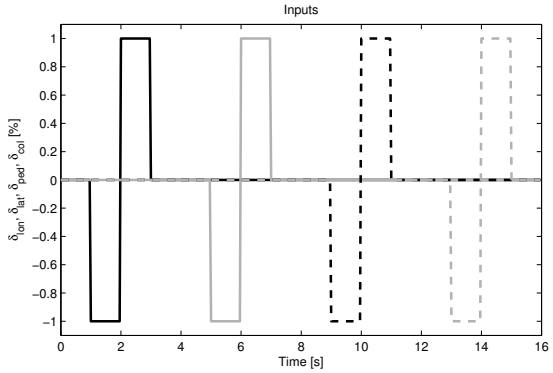

Fig. 1 Doublet input signal used for model validation.

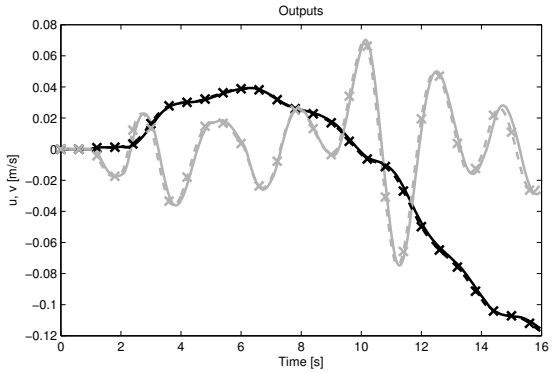

Fig. 2 Doublet output signals (real: solid line; black-box: dashed line; gray-box: cross).

$$RMS = \sqrt{\frac{1}{N}\sum_{i=1}^{N}(y(i)-\hat{y}(i))^2}, \tag{39}$$

where y is the real output and $\hat{y}$ is the estimated one, its value is below 0.01 on all the considered output variables as shown in Table 3. Note that most of the error is due the unestimated input delays, as can be seen in Figure 2.

Finally, in Figures 3-14 the magnitude of the frequency response of the error transfer function defined as

$$E_s(s) = G_s(s;\lambda^0) - G_s(s;\hat{\lambda})$$

is shown, where $G(s;\lambda^0)$ is the true transfer function of the BO-105 model and $G_s(s;\hat{\lambda})$ is the gray-box estimated one. As can be seen from the figures, the magni-

Output	$RMS_{CT-PBSID_o}$	$RMS_{Gray-Box}$
u	0.0013	0.0013
v	0.0044	0.0044
w	0.0026	0.0026
p	0.0002	0.0002
q	0.0003	0.0003
r	0.0003	0.0003
a_x	0.0013	0.0013
a_y	0.0017	0.0017
a_z	0.0077	0.0077
ϕ	0.0001	0.0001
θ	0.0001	0.0001

Table 3 Relative errors norm.

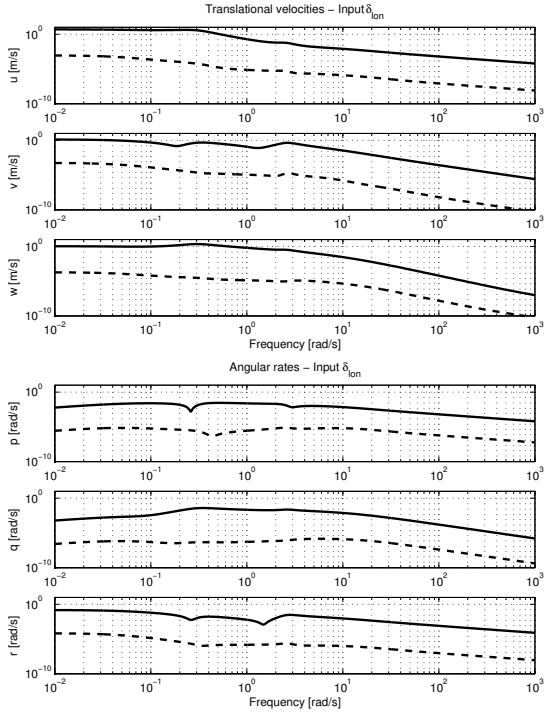

Fig. 3 Frequency response from longitudinal input to linear (top) and angular (bottom) velocities. (real: solid line; error: dashed line)

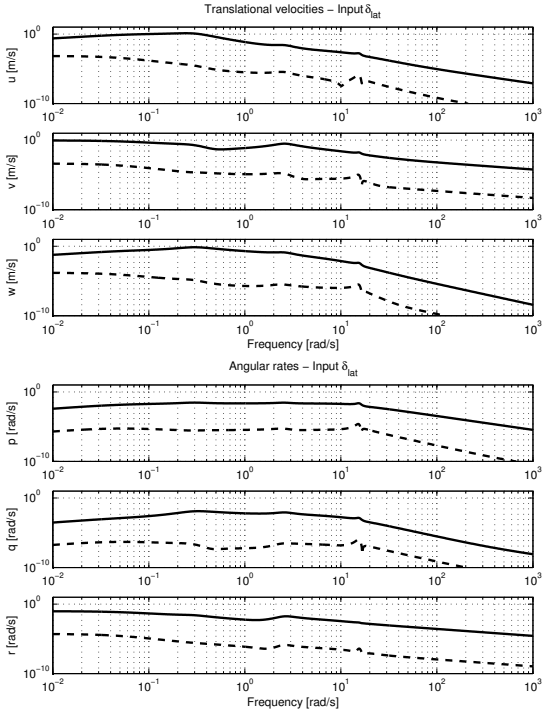

Fig. 4 Frequency response from lateral cyclic input to linear (top) and angular (bottom) velocities. (real: solid line; error: dashed line)

tude of the error frequency response is always several orders of magnitude smaller than the one for the true transfer function.

5 Concluding remarks

The problem of rotorcraft system identification has been considered and a two step technique combining the advantages of time domain and frequency domain methods has been proposed. A simulation study based on a model of the BO-105 helicopter has been used to illustrate the proposed approach. Simulation results show that the proposed schemes are viable for rotorcraft applications and can deal successfully with data generated during closed-loop experiments. Future work will focus on the analysis of the impact on the solution of (35) of an identified model that has been obtained under noisy conditions.

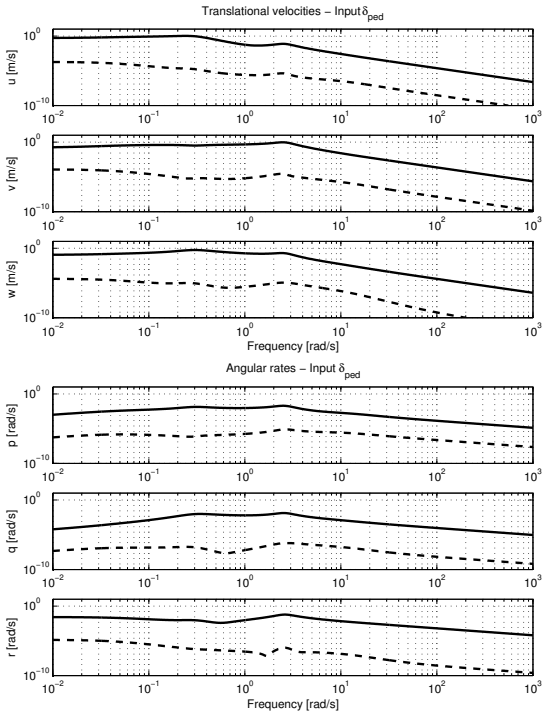

Fig. 5 Frequency response from pedal cyclic input to linear (top) and angular (bottom) velocities. (real: solid line; error: dashed line)

References

1. P. Apkarian and D. Noll. Nonsmooth H_∞ synthesis. *IEEE Transactions on Automatic Control*, 51(1):71–86, 1996.
2. M. Bergamasco. *Continuous-time model identification with applications to rotorcraft dynamics*. PhD thesis, Politecnico di Milano, 2012.
3. M. Bergamasco and M. Lovera. Recovering structured models from unstructured ones: an H_∞ approach. (submitted).
4. M. Bergamasco and M. Lovera. Continuous-time subspace identification in closed-loop. In *19th International Symposium on Mathematical Theory of Networks and Systems, Budapest, Hungary*, 2010.
5. M. Bergamasco and M. Lovera. Continuous-time predictor-based subspace identification for helicopter dynamics. In *37th European Rotorcraft Forum, Gallarate, Italy*, 2011.
6. M. Bergamasco and M. Lovera. Continuous-time predictor-based subspace identification using Laguerre filters. *IET Control Theory and Applications*, 5(7):856–867, 2011. Special issue on Continuous-time Model Identification.
7. S. Bittanti and M. Lovera. Identification of linear models for a hovering helicopter rotor. In *Proceedings of the 11th IFAC Symposium on system identification, Fukuoka, Japan*, 1997.
8. S. Bittanti and M. Lovera. Bootstrap-based estimates of uncertainty in subspace identification methods. *Automatica*, 36(11):1605–1615, 2000.
9. A. Chiuso and G. Picci. Consistency analysis of certain closed-loop subspace identification methods. *Automatica*, 41(3):377–391, 2005.

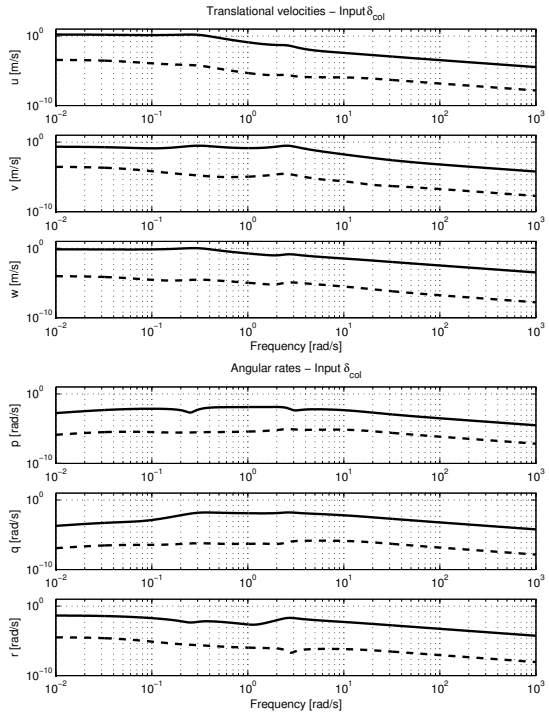

Fig. 6 Frequency response from collective input to linear (top) and angular (bottom) velocities. (real: solid line; error: dashed line)

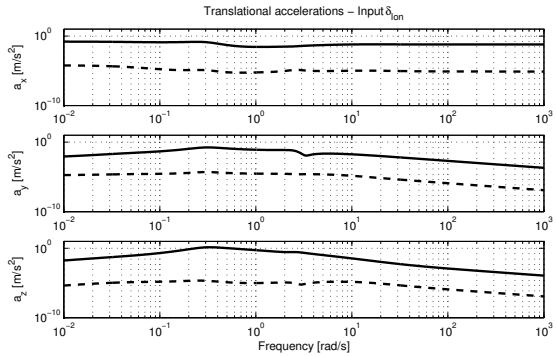

Fig. 7 Frequency response from longitudinal input to linear accelerations. (real: solid line; error: dashed line)

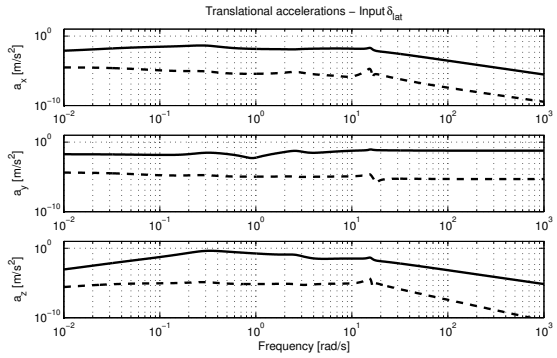

Fig. 8 Frequency response from lateral cyclic input to linear accelerations. (real: solid line; error: dashed line)

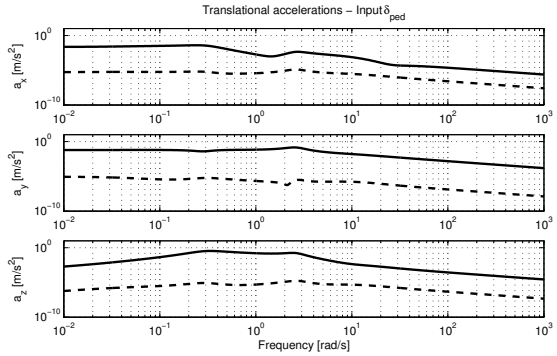

Fig. 9 Frequency response from pedal cyclic input to linear accelerations. (real: solid line; error: dashed line)

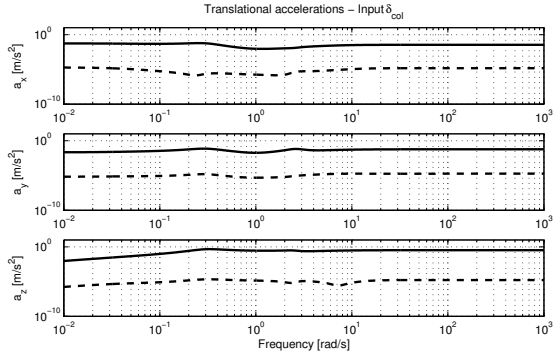

Fig. 10 Frequency response from collective input to linear accelerations. (real: solid line; error: dashed line)

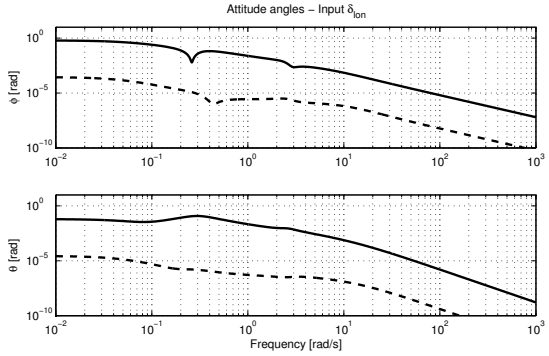

Fig. 11 Frequency response from longitudinal input to attitude angles. (real: solid line; error: dashed line)

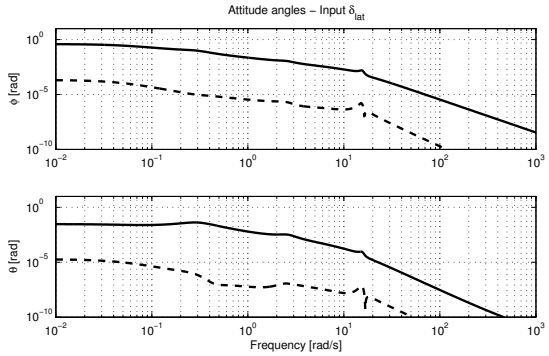

Fig. 12 Frequency response from lateral cyclic input to attitude angles. (real: solid line; error: dashed line)

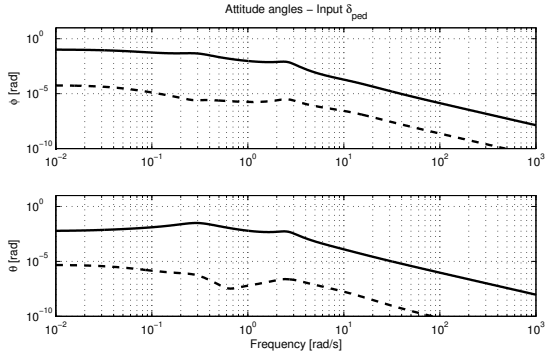

Fig. 13 Frequency response from pedal cyclic input to attitude angles. (real: solid line; error: dashed line)

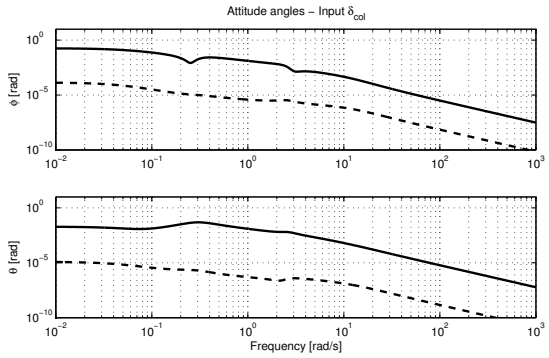

Fig. 14 Frequency response from collective input to attitude angles. (real: solid line; error: dashed line)

10. P. Gahinet and P. Apkarian. Decentralized and fixed-structure H_∞ control in matlab. In *50th IEEE Conference on Decision and Control and European Control Conference, Orlando, USA*, 2011.
11. B. Huang, S.X. Ding, and S.J. Qin. Closed-loop subspace identification: an orthogonal projection approach. *Journal of Process Control*, 15(1):53–66, 2005.
12. R. Jategaonkar. *Flight Vehicle System Identification*. AIAA, 2006.
13. R. Johansson, M. Verhaegen, and C.T. Chou. Stochastic theory of continuous-time state-space identification. *IEEE Transactions on Signal Processing*, 47(1):41–51, 1999.
14. Y. Kinoshita and Y. Ohta. Continuous-time system identification using compactly supported filter kernels generated from Laguerre basis functions. In *49th IEEE Conference on Decision and Control, Atlanta, USA*, 2010.
15. P. Li and Postlethwaite I. Subspace and bootstrap-based techniques for helicopter model identification. *Journal of the American Helicopter Society*, 56(1):012002, 2011.
16. M. Lovera. Identification of MIMO state space models for helicopter dynamics. In *13th IFAC Symposium on System Identification, Rotterdam, The Nederlands*, 2003.
17. Y. Ohta. Realization of input-output maps using generalized orthonormal basis functions. *Systems & Control Letters*, 22(6):437–444, 2005.
18. Y. Ohta. System transformation of unstable systems induced by a shift-invariant subspace. In *50th IEEE Conference on Systems and Control*, 2011. Submitted.
19. Y. Ohta and T. Kawai. Continuous-time subspace system identification using generalized orthonormal basis functions. In *16th International Symposium on Mathematical Theory of Networks and Systems, Leuven, Belgium*, 2004.
20. M. Tischler and M. Cauffman. Frequency-response method for rotorcraft system identification: Flight applications to BO-105 coupled rotor/fuselage dynamics. *Journal of the American Helicopter Society*, 37(3):3–17, 1992.
21. M. Tischler and R. Remple. *Aircraft And Rotorcraft System Identification: Engineering Methods With Flight-test Examples*. AIAA, 2006.
22. P. Van Overschee and B. De Moor. *Subspace identification: theory, implementation, application*. Kluwer Academic Publishers, 1996.
23. M. Verhaegen. Identification of the deterministic part of MIMO state space models given in innovations form from input-output data. *Automatica*, 30(1):61–74, 1994.
24. M. Verhaegen and A. Varga. Some experience with the MOESP class of subspace model identification methods in identifying the BO105 helicopter. Technical Report TR R165-94, DLR, 1994.
25. M. Verhaegen and V. Verdult. *Filtering and System Identification: A Least Squares Approach*. Cambridge University Press, 2007.
26. K. Zhou, J. Doyle, and K. Glover. *Robust and optimal control*. Prentice Hall, 1996.